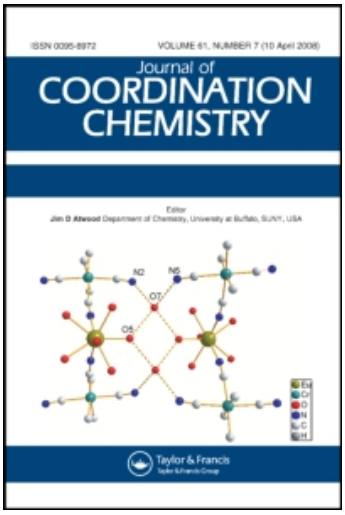

Journal of Coordination Chemistry
Publication details, including instructions for authors and subscription information:
http://www.informaworld.com/smpp/title~content=t713455674

A vic-dioxime ligand bearing fluorescent coumarin moieties and its complexes; preparation, spectroscopy, and electrochemistry

A. Asli Esenpinar[a]; Mehmet Kandaz[b]; Alİ Riza Özkaya[a]; Mustafa Bulut[a]; Orhan Güney[c]
[a] Department of Chemistry, Marmara University, Istanbul, Turkey [b] Department of Chemistry, Sakarya University, Sakarya, Turkey [c] Department of Chemistry, Istanbul Technical University, Istanbul, Turkey

First published on: 19 September 2007

To cite this Article Esenpinar, A. Asli , Kandaz, Mehmet , Özkaya, Alİ Riza , Bulut, Mustafa and Güney, Orhan(2008) 'A vic-dioxime ligand bearing fluorescent coumarin moieties and its complexes; preparation, spectroscopy, and electrochemistry', Journal of Coordination Chemistry, 61: 8, 1172 — 1183, First published on: 19 September 2007 (iFirst)
To link to this Article: DOI: 10.1080/00958970701502342
URL: http://dx.doi.org/10.1080/00958970701502342

Journal of Coordination Chemistry
Vol. 61, No. 8, 20 April 2008, 1172–1183

A *vic*-dioxime ligand bearing fluorescent coumarin moieties and its complexes; preparation, spectroscopy, and electrochemistry

A. ASLI ESENPINAR†, MEHMET KANDAZ*‡, ALİ RIZA ÖZKAYA†, MUSTAFA BULUT† and ORHAN GÜNEY§

†Department of Chemistry, Marmara University, 34722 Kadıköy, Istanbul, Turkey
‡Department of Chemistry, Sakarya University, 541400, Serdivan, Sakarya, Turkey
§Department of Chemistry, Istanbul Technical University, 34469, Maslak, Istanbul, Turkey

(*Received 31 January 2007; in final form 30 March 2007*)

The synthesis of a new *vic*-dioxime ligand, N,N'^2-dihydroxy-O^1,O^2-*bis*(4-methyl-2-oxo-2H-chromen-7-yl)oxalimidamid (LH_2) (**1**), bearing functional coumarins and its soluble mono- {Ni(II), Cu(II), Co(II)} and dinuclear {UO_2(II)} complexes are presented. The fluorescence properties due to the 7-hydroxy-4-methylcoumarin fluorophore, which is conjugated with *vic*-dioxime that functions as the MN_4 core of **1** and its complexes, are also reported. The formation of coordination complexes resulted in the blue shift in excitation spectrum and fluorescence quenching of **1**. Both mononuclear {$(LH)_2$M, M=Ni(II), Cu(II), and Co(II)} and homodinuclear {$(LH)_2(UO_2)_2(OH)_2$)} complexes have been obtained with metal : ligand ratios of 1 : 2 and 2 : 2, respectively. The characterizations of the new compounds were made by elemental analysis, ^{1}H-NMR, FT-IR, UV-Vis, and LCMS data. Redox behavior of **1**, involving oxime and coumarin moieties, and its complexes with Ni(II), Cu(II), Co(II) and UO_2(II) were investigated by cyclic voltammetry. The comparison of the electrochemical behavior of **1** with its complexes enabled us to identify metal-, oxime- and coumarin-based signals.

Keywords: *Vic*-dioxime complexes; Coumarin; Fluorescence; Nickel; Copper; Cobalt; Uranyl; Cyclic voltammetry

1. Introduction

Vic-dioximes have attracted interest due to their applications in various chemical processes [1–3]; coumarin derivatives exhibiting useful and diverse activity in pharmaceuticals, fragrances, agrochemicals, insecticides and polymer science have become the most extensively investigated and commercially significant group of organic fluorescent materials in recent years [4–7]. Coumarins also play a vital role in electrophotographic and electroluminescent devices and laser dyes [7, 8]. Thus, attachment of coumarin moieties on a *vic*-dioxime could lead to new coumarin

*Corresponding author. Fax: + 90 264 295 59 50. Email: mkandaz@sakarya.edu.tr

ISSN 0095-8972 print/ISSN 1029-0389 online © 2008 Taylor & Francis
DOI: 10.1080/00958970701502342

derivatives extending the available range of long wavelength emitting fluorescent materials [9]. Considerable effort has been made to incorporate functional groups on the periphery of the *vic*-dioxime molecule to modify its conformational, optical and redox properties [10–12].

Although various *vic*-dioxime complexes involving different peripheral donor atoms have been synthesized and characterized [13–16], ones with peripheral fluorescent substituents have not been studied to the best of our knowledge.

The stability of the oxidation states of the metal center in oxime-metal complexes depends on the metal coordination environment [17]. The ability of donor atoms to stabilize reduced and/or oxidized forms of metal is important for their role in bioinorganic systems [17]. Hence, the investigation of redox properties has importance for a better understanding of their properties.

In this study, we report the synthesis and spectroscopic characterization of a new fluorescent chemosensor ligand containing both coumarin and *vic*-dioxime and its transition metal complexes. The electrochemical properties of the compounds were also studied by cyclic voltammetry.

2. Results and discussion

2.1. *Materials and equipment*

N'^2-Dihydroxy-O^1,O^2-*bis*(4-methyl-2-*oxo*-2H-chromen-7-yl)oxalimidamid (LH_2) (**1**) was prepared by reaction between 7-hydroxy-4-methylcoumarin fluorophore and (*E,E*)-dichloroglyoxime in the presence of Na_2CO_3. The stepwise synthesis of **1** and its complexes are depicted in scheme 1 and figure 1. This compound is soluble in DMF, DMSO, quinoline, pyridine, DMAA and insoluble in MeOH, EtOH, $CHCl_3$, MeCN and THF. The syntheses of mononuclear complexes [$(LH)_2M$] [M = Ni (II) (**2**), Cu(II) (**3**), Co(II) (**4**)] (scheme 1) and dinuclear complex [$(LH)_2(UO_2)_2(OH)_2$] (**5**) (figure 1) were achieved at room temperature using a metal/ligand molar ratio 1 : 2 for the mononuclear and 2 : 2 for the dinuclear substituted *vic*-dioxime complexes. These products were isolated as analytically pure species *via* spontaneous precipitation. Further precipitation was achieved by adding triethylamine to the crude product after the first precipitation [10–15, 18, 20–23].

The colors, yields and elemental analysis of **1** and its complexes are listed in table 1. The IR bands have the simplest diagnostic information for the formation of **1** and its complexes. Therefore, the presence or absence of certain bands of the complexes compared to those of **1** in the IR spectra has been utilized to establish the nature of the complexes. In the IR spectrum of **1** the ν(–NOH), ν(C=N) and ν(N–O) stretching vibrations are observed at 3321, 1502, and 1027 cm^{-1}, respectively. Formation of *vic*-dioxime complexes are shown by disappearance of the sharp intense ν(–NOH) stretching vibration band at 3321 cm^{-1}, shifts in the ν(C=N) stretching and ν(N–O) bending bands to lower or higher frequencies, and the appearance of the broad (O–H $\cdots$ O) deformation vibration at ca 1700–1725 cm^{-1} due to hydrogen bonding upon complexation. These features are also indicative of N,N′-chelation in the metal complexes. The remaining absorptions of **2** and **4** are very similar to **1** with small shifts in frequency. The ν(N–OH), ν(N–O), and ν(O=U=O) vibrations at 3433,

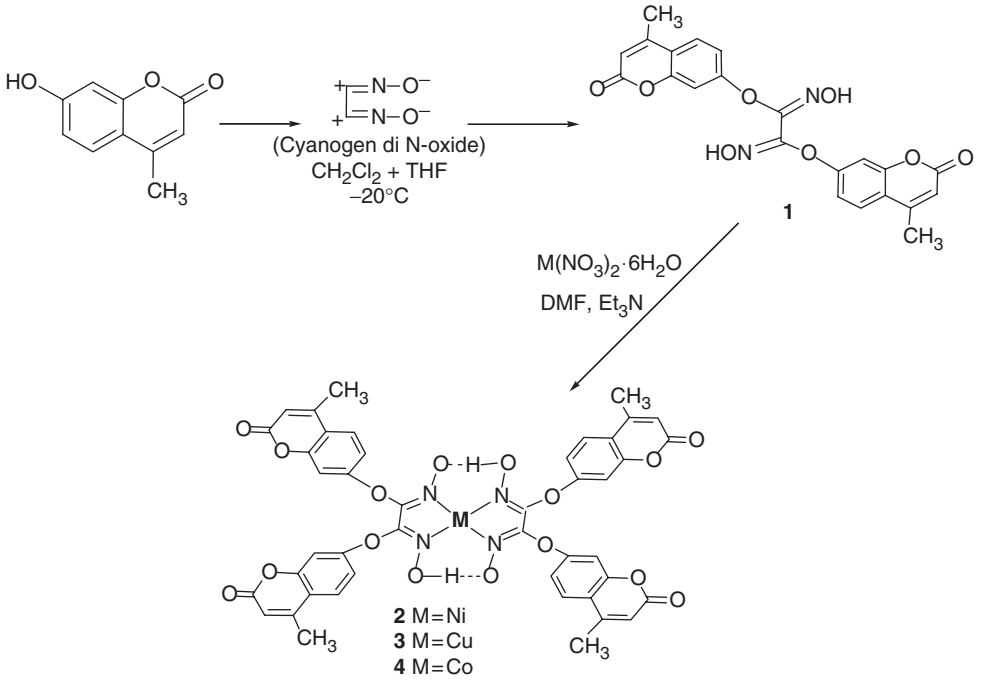

Scheme 1. (i) MeOH, DCGO, Reflux, $NaHCO_3$; (ii) $ML_2X \cdot 6H_2O$ ($M = Ni^{II}$, Cu^{II}, Co^{II}). X: NO_3^-; Et_3N, THF.

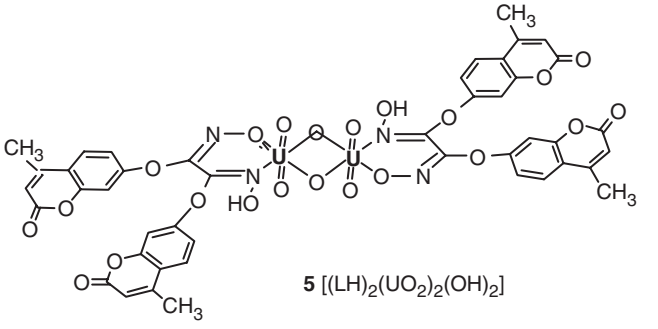

Figure 1. Binuclear uranyl complex (**5**).

1068 and 864 cm^{-1} of dinuclear $[(LH)_2(UO_2)_2(OH)_2]$ were observed as strong broad bands. While weak (O–H $\cdots$ O) deformations of all mono complexes are observed at around 1700 cm^{-1}, these vibrations are not involved in the IR spectra of the dinuclear uranyl complex.

In the ^{1}H-NMR spectrum of **1** in DMSO-d_6, a singlet at $\delta = 12.34$ (s, 2H, D_2O-exchangeable) is assigned to =N–OH. Four different H atoms on the coumarin moieties were easily determined by NMR spectroscopy. The existence of diamagnetic **2** was identified by the disappearance of the N–OH signal at 12.34 ppm in **1**. Intramolecular deuterium-exchangeable H-bridge protons were observed at lower field, $\delta = 15.92$ ppm. Consequently, it may be concluded that Ni(II) (d^8) is coordinated with

the dioximate in square planar geometry [10–12, 18, 24]. The ^{1}H-NMR signal for the coumarin moieties were similar to **1** except for a slight shift.

The IR spectrum of the uranyl complex is consistent with the dimeric structure. As expected, the (*E,Z*)-[$(LH)_2(UO_2)_2(OH)_2$] (**5**) complex has a tedrahedral and paramagnetic structure and its NMR signals are broad. The NMR spectrum of **5** contain two peaks for N–OH corresponding to oxime group in low field ($\delta = 12.35$, 12.32 ppm, s, 2H, N–OH, D-exchangeable), which can be attributed to the magnetic anisotropy of the uranyl ion as discussed previously in reports of the Bekaroğlu group and our work [10–13, 18, 24]. Uranyl ions enhance the chemical shift differences between non-equivalent protons.

Elemental anaylses, LSMS and AAS confirmed mononuclear complexation with Ni(II), Cu(II) and Co(II) and dinuclear complexation with UO_2(II).

2.2. *Absorption spectra*

Absorption spectra of **1** and its mononuclear complexes were measured to understand the effects of different transition metal ions on the optical properties (figure 2).

Table 1. Analytical and physical data for **1** and its complexes.

Compounds	Colour	Calcd (Found)%		
		C	H	N
(**1**) LH_2	Brown	60.55 (60.01)	3.66 (3.57)	6.42 (6.13)
(**2**) $(LH)_2Ni$ (E,E)	Reddish-brown	56.83 (56.34)	3.22 (3.18)	6.02 (5.88)
(**3**) $(LH)_2$ Cu	Brown	56.53 (56.27)	3.21 (3.04)	5.99 (5.77)
(**4**) $(LH)_2$ Co	Dark-brown	56.83 (56.54)	3.22 (3.21)	6.02 (5.95)
(**5**) $(LH)_2(UO_2)_2(OH)_2$	Orange	36.56 (36.70)	2.07 (2.20)	3.87 (3.58)

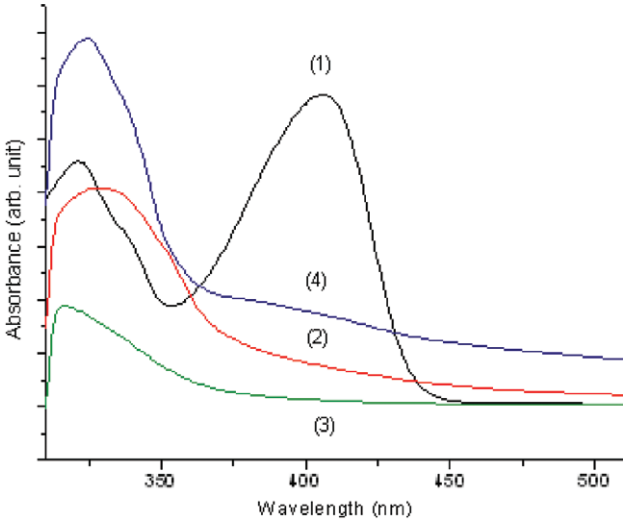

Figure 2. Absorption spectra of LH_2 (**1**) and its complexes with Ni^{2+} (**2**), Cu^{2+} (**3**) and Co^{2+} (**4**) in DMF.

1 exhibits absorption maximum at 410 nm. The peak at longest wavelength corresponds to HOMO–LUMO transitions and the maximum absorption wavelength of the compounds originates from the HOMO to LUMO electron transition. The width of the optical gap is between the ground electron level (HOMO) and the lowest unoccupied level (LUMO). The optical gap value of **1** was calculated to be 3.02 eV. Since the metal ion complexes of **1** exhibit broad and structureless absorption spectra at longest wavelength, the optical gap values were calculated, using maximum excitation intensity values at longest wavelengths, as 3.04 eV for Ni(II), 3.29 eV for Cu(II) and 3.58 eV for Co(II) complexes of **1**.

2.3. *Fluorescence measurements*

Compound **1** exhibits maximum intensity in excitation wavelength at 410 nm (figure 3a). From studying molecular orbitals, we see that the excitation to the first excited state is mainly a HOMO to LUMO transition. HOMO and LUMO are

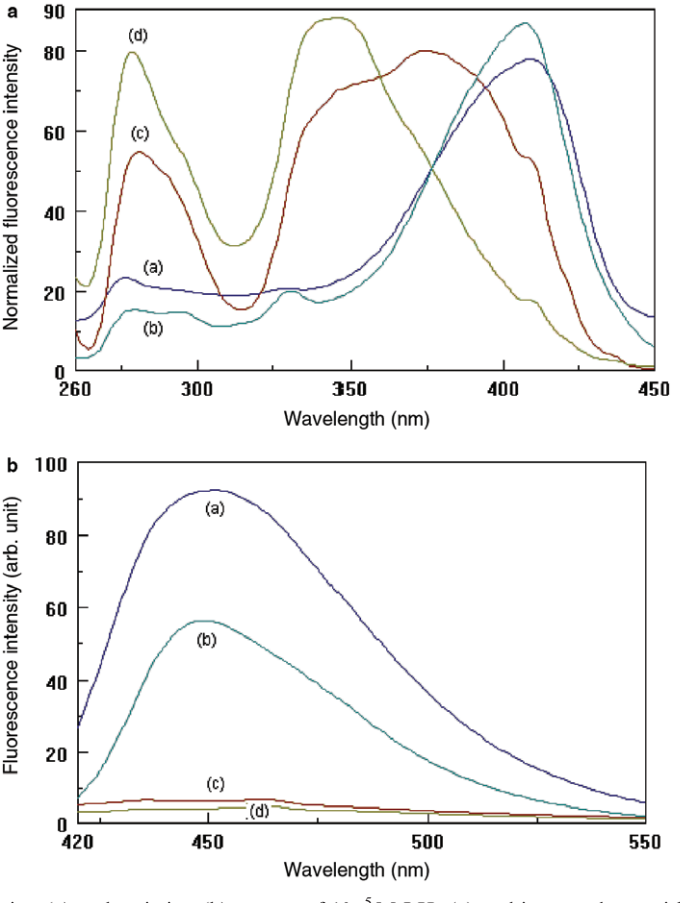

Figure 3. Excitation (a) and emission (b) spectra of 10^{-5} M LH_2 (a) and its complexes with Cu^{2+} (b), Ni^{2+} (c) and Co^{2+} (d) ions in DMF. Excitation and emission slit widths set at 5 nm.

delocalized orbitals, but HOMO tends to localize to the **1** donor units and LUMO to the acceptor orbital of the metal ion. We typically see a blue-shift (peaks move towards shorter wavelength) as the LH_2 forms complex with metal ion. This shift is 3 nm for Ni(II), 34 nm for Cu(II) and 64 nm for Co(II) complex. Connecting d-orbital of metal ion leads to a larger set of molecular orbitals, resulting in an increase of the LUMO and a lowering of the HOMO energy. The result is an increase of the bandgap and higher excitation energies. We observe that the peak, corresponding to the lowest excitation, is more blue-shifted than the peak for higher excitation, for metal ion with fewer d electrons. Decrease in excitation intensity is observed depending on complex formation with metal ions in the order Ni(II) < Cu(II) < Co(II).

When excited at 410 nm **1** shows an emission maximum at 449 nm, which does not shift upon binding to transition metal ions (figure 3b). From this figure, it is evident that fluorescence emission intensity of **1** decreases dramatically on complex formation with transition metal ions. These coordination complexes make possible energy transfer from the excited state of **1** to metal ions increasing the non-radiative transitions and decreasing the fluorescence emission. Decrease in emission maxima were in the order of Ni(II) < Cu(II) < Co(II) complexes of **1**.

2.4. *Electrochemical measurements*

The electrochemical properties of **1**–**5** were investigated using voltammetric techniques in DMSO/TBAP with a platinum working electrode. The results are summarized in table 2. With controlled potential coulometry studies, complete electrolysis of the

Table 2. Voltammetric data for **1**, **2**, **3**, **4** and **5** in DMSO/TBAP.[a]

Compound	Redox couple	$E_{1/2}$ or E_p (*V*)[b]	ΔE_p (V)[c]
1	Ox/Ox^+ (I)	0.78	–
	Ox/Ox^- (IV)	−1.52	–
	$Coum/Coum^-$ (V)	−1.62	0.20
2	Ox/Ox^+ (I)	0.76	–
	Ni(II)/Ni(III) (II)	0.52	–
	Ni(II)/Ni(I) (III)	−0.70	0.22
	Ox/Ox^- (IV)	−1.18	–
	$Coum/Coum^-$ (V)	−1.74	–
3	Cu(II)/Cu(III) (II)	0.14	0.06
	Cu(II)/Cu(0) (III)	−0.07	0.03
	Ox/Ox^- (IV)	−1.07	–
	$Coum/Coum^-$ (V)	−1.60	0.12
4	Co(II)/Co(III) (II)	0.62	0.06
	Co(II)/Co(I) (III)	−0.80	0.24
	Ox/Ox^- (IV)	−1.34	0.10
	$Coum/Coum^-$ (V)	−1.74	0.22
5	Ox/Ox^+ (I)	0.56	0.14
	$U(VI)O_2/U(V)O_2$ (III)	−0.73	0.16

[a]Half-wave ($E_{1/2}$) or peak (E_p) potentials in DMSO/TBAP *vs.* Fc/Fc^+ couple correspond approximately with the above data minus 0.50 V. These data were measured by cyclic voltammetry.

[b]$E_{1/2} = (E_{pa} + E_{pc})/2$ for reversible or quasi-reversible processes. E_p indicates the cathodic peak potential for irreversible reduction processes and the anodic peak potential for irreversible oxidation processes.

[c]The peak separation ($\Delta E_p = E_{pa} - E_{pc}$) values are reported at 0.050 Vs^{-1}.

solution at the working electrode at constant potential (E_{pc} of redox couple) was achieved, the time integration of the electrolysis current was recorded and the charge, Q, at the end of electrolysis was calculated using the current-time response. *Faraday*'s law was used to estimate the number of electrons transferred. The number of electrons was found to be two for the first reduction processes of **2** and **5** and one for all other redox processes.

First, we carried out voltammetric measurements of **1** in order to compare its redox behavior with those of the metal complexes **2**–**5**. Figure 4 indicates the cyclic voltammogram of **1**, which displays two one-electron reductions and a one-electron oxidation process (table 2). Comparison of the redox data of **1** with previously reported oxime-metal complexes [10, 25] imply that the first oxidation and the first reduction processes probably correspond to the oxime moieties, while the second reduction is from the coumarin moieties. The oxime-based processes are irreversible, while the coumarin-based second reduction process has a quasi-reversible character with a peak separation of 0.18 V. Although the first oxidation process (couple I) was recorded as an ill-defined signal during the CV measurement, it was detected by differential pulse voltammetry (figure 4).

Figure 5 indicates the cyclic voltammograms of **3** at different scan rates on a platinum working electrode in DMSO/TBAP. Complex **3** displays three reductions and an oxidation (table 2). The first reduction (couple III) is a two-electron process with a peak separation of 0.030 V, and may be assigned to Cu(II)/Cu(0); one-electron first oxidation couple (couple II) is probably Cu(II)/Cu(III). The anodic peak of couple III is observed only at low scan rates; the anodic peaks of couples II and III are separate at low scan rates, but overlap at high scan rates (A in figure 5). The direct proportionality of the anodic peak current of the composite couple with the scan rate suggests oxidation of electro-active species directly from the electrode surface. Probably, Cu(0) deposited on the platinum electrode during the cathodic scan is first oxidized to Cu(II) and then to Cu(III) during the reverse scan. It appears that Cu(I) is unstable towards conversion

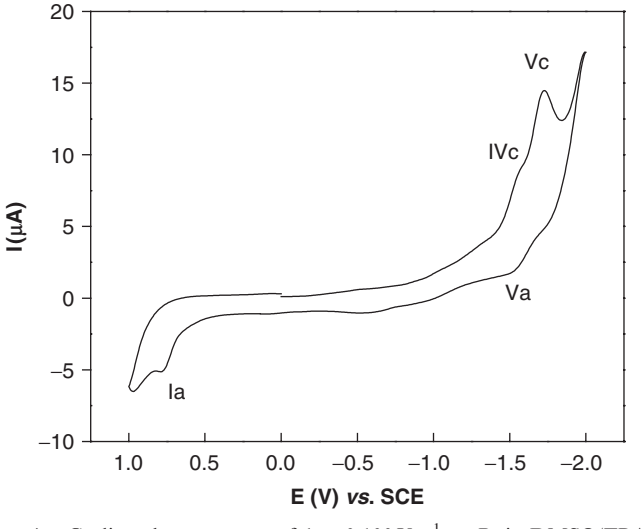

Figure 4. Cyclic voltammogram of **1** at 0.100 Vs^{-1} on Pt in DMSO/TBAP.

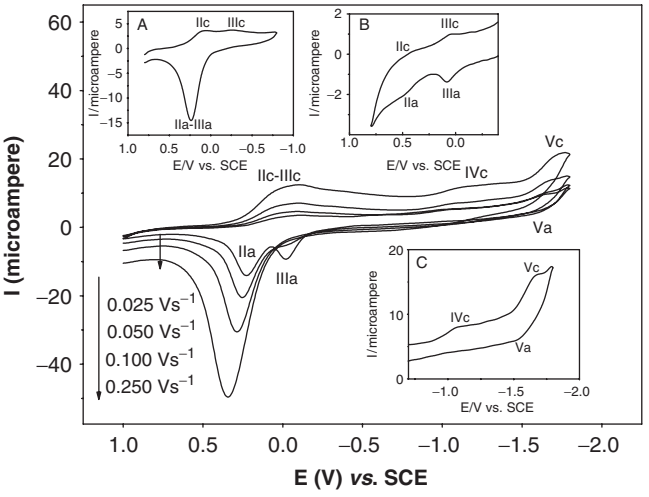

Figure 5. Cyclic voltammograms of **3** at various scan rates on Pt in DMSO/TBAP. Scan rate: 0.100 V s^{-1}, scan range: (+0.8)–(−0.8) V for inset A. Inset B indicates cyclic voltammogram of **3** at 0.100 V s^{-1} on GCE in DMSO/TBAP. Scan rate: 0.100 V s^{-1}, scan range: (−0.7)–(−1.8) V for inset C.

to Cu(0) which tends to plate out on the electrode surface, as also reported previously [17]. This behavior was not observed when the platinum working electrode was replaced with a glassy carbon working electrode (B in figure 5). The couples II and III were well separated at all scan rates, as shown for 0.050 Vs^{-1} in figure 5B. The voltammetric behavior on platinum working electrode through scans between 0.40–1.00 V was nearly identical to that through the full scan starting at 1.0 V. In the case of glassy carbon electrode, it appears that electrochemically reduced species involving Cu(I) are stable, and thus the first reduction (couple III) corresponds to Cu(II)/Cu(I) process without decomposition of the complex. Diffusion-controlled nature of the first oxidation process of **3** [Cu(II)/Cu(III), couple II)], i.e., direct proportionality of the peak currents with the square root of scan rate, provided evidence for assignment of these processes. The comparison of the voltammetric data of **3** with that of **1** suggests that the second and third reductions (IV and V) are oxime- and coumarin-based processes, respectively (figure 5 and inset C in figure 5). These ligand-based reduction processes, especially the oxime-based reduction of **3** (couple IV) occur at potentials less negative than those of **1**. This was also observed with **2** and **4**, presumably due to negative charge transfer from ligand to metal during the formation of metal complexes.

The redox chemistry of Ni(II) (**2**) and Co(II) (**4**) complexes exhibited both M(II)/M(III) and M(II)/M(I) redox couples. In the cyclic voltammograms of **2** and **4**, first reduction and first oxidation processes for these complexes take place on the metal center; voltammetric data is given in table 2. It is clear in the literature that oxime-containing metal complexes give redox signals involving both higher and lower oxidation states of the metal depending on the coordination environment of the metal [10, 17, 25, 26]. For both **2** and **4**, the second reduction process corresponds to the oxime. Complex **2** also showed a one-electron irreversible process (I) which can be assigned to the oxidation of oxime moieties, while coumarin-based redox processes were not observed. The third reduction process of **4** can be assigned to coumarin moieties.

As observed for **3**, the ligand-based reduction processes of **2** and **4** occur at potentials less negative than those of **1**.

Complex **5** displays a two-electron quasi-reversible reduction couple (III) at $E_{1/2} = -0.73$ V assigned to $U^{VI}O_2/U^{V}O_2$ and a one-electron quasi-reversible oxidation couple (I) at $E_{1/2} = 0.56$ V, which can be assigned to the oxidation of oxime moieties since oxidation of UO_2 is not possible.

3. Experimental

3.1. *Synthesis*

(*E,E*)-Dichloroglyoxime and 7-hydroxy-4-methylcoumarin were prepared by reported procedures [27–29]. All reagents and solvents were of reagent-grade quality, obtained from commercial suppliers and used without further purification. Mass spectra were recorded on a Varian 711 and VG Zapspec spectrometer. The IR spectra were recorded on a Shimadzu Fourier Transform FTIR-8300 infrared spectrophotometer using KBr pellets. Electronic spectra were recorded on a Shimadzu UV-1601 UV-Visible spectrophotometer. Fluorescence spectra were obtained on a Jasco FP-750 spectrofluorometer. The emission and excitation spectra of **1** and its complexes were measured in DMF solution. ^{1}H-NMR spectra were recorded on a Bruker 250 MHz spectrometer. Elemental analysis (C, H, and N) was performed at the Instrumental Analysis Laboratory of Marmara University. Metal content was determined with a Hitachi 180–80 atomic absorption spectrometer in solution prepared by decomposition of the compounds in aqua regia followed by dilution with water.

Tetrabutylammonium perchlorate (TBAP) (electrochemical grade, Fluka Chemical Co.) as the supporting electrolyte and extra pure dimethylsulfoxide (DMSO) (Fluka Chemical Co.) as the solvent were used in electrochemical measurements. Electrochemical measurements were carried out with a Princeton Applied Research Model Versostat II potentiostat/galvanostat, controlled by an external PC, utilizing a three electrode configuration at 25°C. A saturated calomel electrode (SCE) was employed as the reference electrode. A platinum spiral wire was used as the auxiliary electrode. The working electrode was platinum with an area of 0.12 cm^2 in the measurements. The surface of the platinum working electrode was polished with a H_2O suspension of Al_2O_3 before each run. The last polishing was done with a particle size of 50 nm. The ferrocene/ferrocenium couple (Fc/Fc^+) was used as an internal standard. Solutions were deoxygenated by a stream of high-purity nitrogen for at least 15 min prior to running the experiment and the solution was protected from air by a blanket of nitrogen during the experiment. For the controlled-potential coulometry (CPC) studies, a platinum gauze working electrode, a platinum wire counter electrode separated with a bridge, a SCE as reference electrode, and a model 377/12 synchronous stirrer were used.

3.2. *N'^1,N'^2-dihydroxy-O^1,O^2-bis(4-methyl-2-oxo-2H-chromen-7-yl) oxalimidamid (LH_2) (1)*

20 cm^3 solution of 0.22 g (*E,E*)-dichloroglyoxime (1.40 mmol) in dry EtOH was added dropwise to a 20 cm^3 mixture of 7-hydroxy-4-methylcoumarin (0.5 g, 2.84 mmol) and

0.47 g of anhydrous $NaHCO_3$ (excess) in absolute DMF, which was stirred at RT for 0.5 h under N_2. The mixture was stirred at room temperature for 1 h. The color of the solution turned light yellow during the time; the reaction mixture was refluxed for an additional 4 h with stirring. The reaction mixture was allowed to cool at room temperature. After filtration of sodium chloride formed, the volume of the reaction mixture was reduced to dryness and excess coumarin and dichloroglyoxime (DCGO) removed by washing the solution with chloroform and cold THF. The red oily product was dried *in vacuo* at room temperature. This compound is soluble in DMF, DMSO and MeOH, and insoluble in $CHCl_3$, CH_2Cl_2, and THF.

Yield: 0.048 g (78%). M.p.: oily, FT-IR ν_{max} (cm^{-1}, thin film): 3321 (N–OH), 3021 (Ar–H), 2978–2870 (Aliph–H), 1734 (w, O–H $\cdots$ O), 1691 (C=O), 1595 (C=C), 1502 (C=N), 1291 (Ar–O–C), 1027 (N–O). ^{1}H-NMR (d_6-DMSO, 300 MHz) δ: 12.34 (s, 2H, =N–OH, D_2O-exchangeable), 7.60 (dd, 2H, Ar–H), 7.26 (dd, 2H, Ar–H, ortho to CH_3Ar), 7.10 (s, 2H, Ar–H, ortho to Ar–O–), 6.55 (dd, Ar–H, 2H, ortho to –COO), 2.40 (s, 6 H, $-CH_3$) ppm. UV-Vis (in DMF) λ_{max}/nm (log ε): 400 (5.05), 317 (4.95). MS (LSMS, scan ES^+): m/z (%) = 435.2(12) $[M+1]^+$, 455.39(5) $[M+Na]^+$, 433.24(50), 419.22(20), 413.46(30), 403.26(55), 394.32(100), 389.31(45), 251.21(7), 214.23(100), 173.20(20), 157.05(40).

3.3. *N,N′-coordinated complexes [M(HL)$_2$], M=Ni(II), Cu(II), Co(II) (2, 3 and 4)*

3 cm^3 of the appropriate metal salt solution [$Ni(NO_3)_2 \cdot 6H_2O$ (0.017 g, 0.057 mmol); $Cu(NO_3)_2 \cdot 6H_2O$ (0.017 g, 0.057 mmol); $Co(NO_3)_2 \cdot 6H_2O$ (0.017 g, 0.057 mmol)] in THF was added dropwise with stirring at room temperature to a solution of **1** (0.05 g, 0.12 mmol) (ca 3 cm^3) in DMF. A distinct change in color of the solution was observed. The resulting mixture was then stirred at 60°C for 3 h to complete the reaction. An equivalent of $(C_2H_5)_3N$ in THF was added dropwise to precipitate (*E,E*)-$Ni(LH)_2$, (*E,E*)-$Cu(LH)_2$, and (*E,E*)-$Co(LH)_2$. All the mononuclear complexes separated as powders, collected by filtration, and then washed successively with water, alcohol, THF, acetone and Et_2O to remove unreacted organic and inorganic impurities. The products were dried in a vacuum desiccator over $CaCl_2$. These compounds are soluble in DMF and DMSO and insoluble in MeOH, EtOH, $CHCl_3$, CH_2Cl_2 and THF.

(*E,E*)-Ni(LH)$_2$ (2): Yield: 0.015 g (28%). m.p.: >300°C. FT-IR ν_{max}/cm^{-1}: 3433 (N–OH), 3050 (Ar–H), 3080 (w, Ar–H), 2918–2887 (w, Aliph-H), 1702 (m, O–H $\cdots$ O bridge), 1688 (coumarin C=O), 1550 (C=C), 1502 (C=N), 1295 (Ar–O–C), 1064 (s, N–O). ^{1}H-NMR (d_6-DMSO, 300 MHz) δ: 15.92 (s, 2H, O $\cdots$ H $\cdots$ O, D_2O-exchangeable), 7.88 (dd, 2H, Ar–H), 7.81 (s, 2H, Ar–H, ortho to CH_3 Ar), 7.19 (dd, 2H, Ar–H, ortho to Ar–O–), 6.38 (s, Ar–H, 2H, ortho to –COO), 2.43 (s, 6 H, $-CH_3$). UV-Vis (in DMF) λ_{max}/nm (log ε) = 324 (4.91). MS (LSMS, scan ES^+): m/z (%): 929.33(7) $[(M+H)]^+$, 807.02(5), 705.12(7), 655.54(10), 420.10(15), 312.33(20), 254.04(25), 197(35), 175(55), 157.07(65).

(*E,E*)-Cu(LH)$_2$ (3): 0.02 g (43%); m.p.: >300°C. FT-IR ν_{max}/cm^{-1}: 3425 (N–OH), 3063 (w, Ar–H), 2975–2881 (w, Aliph-H), 1705 (m, O–H $\cdots$ O bridge), 1675 (C=O), 1595 (C=C), 1503 (C=N), 1288 (Ar–O–C), 1072 (N–O). UV-Vis (DMF) λ_{max}/nm = 315 (4.57). MS (LSMS, scan ES^+): m/z (%): 935.13(3) $(M)^+$, 951.02(5), 1003.39(3),

871.99(10), 806.92(5), 740.28(10), 687.22(50), 645.17(100), 606.06(60), 566.27(70), 538.11(50), 453.20(100), 279.19(70), 158.17(55).

(*E*,*E*)-Co(LH)$_2$ (4): Yield: 0.017 g (33%); m.p.: >300°C. ν_{max}/cm^{-1}: 3448 (N–OH), 3052 (Ar–H), 2926–2814 (Aliph-H), 1710 (O–H $\cdots$ O bridge), 1684 (C=O), 1595 (C=C), 1506 (C=N), 1283 (Ar–O–C), 1068 (N–O). UV-Vis (DMF) λ_{max}/nm (log ε) = 321 (5.13). MS (LSMS, scan ES$^+$): *m*/*z* (%): 929.93(3) M$^+$, 817.33(5), 656.06(7), 556.56(10), 479.04(25), 391.07(25), 289.02(50), 254.04(30), 197.10 (40), 175.07(90), 158.27(60).

3.4. *Dinuclear $U^{VI}O_2$ complex [(LH)$_2$(UO$_2$)$_2$(OH)$_2$] (5)*

To a solution 0.05 g of **1** (0.12 mmol) in DMF (3 cm^3), a solution 0.033 g of $UO_2(NO_3)_2(OH)_2$ (0.057 mmol) in 3 cm^3 THF was added. The color of the solution turned orange and the mixture was heated on a water bath for ca 2 h and then at 50–60°C for 2 h. Adding an equivalent of Et_3N to the mixture with stirring gave an orange precipitate. The mixture was cooled to room temperature, filtered, and the residue washed with hot water, EtOH, acetone and Et_2O, and finally dried *in vacuo*. **5** is soluble in DMF and DMSO and insoluble in MeOH, EtOH, $CHCl_3$, CH_2Cl_2 and THF.

Yield: 0.034 g (41%); m.p: >300°C. FT-IR ν_{max}/cm^{-1}: 3433 (N–OH), 3048 (Ar–H), 2988 (Aliph-H), 1651 (C=O), 1599 (C=C), 1506 (st, C=N), 1283 (Ar–O–C), 1068 (N–O), 864 (st, O=U=O). ^{1}H-NMR (d_6-DMSO, 300 MHz) δ: 12.35 and 12.32 (s, broad, 2H, N–OH, D_2O-exchangeable), 7.82 (dd, 2H, Ar–H), 7.38 (dd, 2H, Ar–H, ortho to CH_3Ar), 6.85 (s, 2H, Ar–H, ortho to Ar–O–), 6.40 (dd, Ar–H, 2H, ortho to –COO), 2.42 (s, 6 H, –CH_3). UV-Vis (in DMF) λ_{max}/nm (log ε) = 320 (4.71). MS (LSMS, scan ES$^+$): *m*/*z* (%): 1440.79 M$^+$(5), 502.47(10), 412.40(7), 358.39(7), 286.45(10), 206.07(15), 194.17(20), 160.05(40), 130.09(65).

Acknowledgements

We thank the Research Funds of DPT (Project no: 2004; 2003K120970), Marmara University, and the Scientific and Research Council of Turkey [TBAG-AY/397(104T384)] for financial support.

References

[1] G.A. Melson. *Co-ordination Chemistry of Macrocyclic Compounds*, Plenum Press, New York (1979).
[2] I. Van de Voorde, L. Pinoy, R.F. De Ketelaere. *J. Membr. Sci.*, **234**, 11 (2004).
[3] D.B. Warren, G. Dyson, F. Grieser, J.M. Perera, G.W. Stevens, M.A. Rizzacasa. *Colloid Surfaces A: Physicochem. Eng. Aspects*, **227**, 49 (2003).
[4] S. Xiao, T. Yi, F. Li, C. Huang. *Tetrahedron Lett.*, **46**, 9009 (2005).
[5] A. Gomes, E. Fernandes, J.L.F.C. Lima. *J. Biochem. Biophys. Meth.*, **65**, 45 (2005).
[6] M.A. Saleh, A. Kamel, A. El-Demerdash, J. Jones. *Chemosphere*, **36**, 1543 (1998).
[7] H. Yu, H. Mizufune, K. Uenaka, T. Moritoki, H. Koshima. *Tetrahedron*, **61**, 8932 (2005).
[8] I. Tanaka, Y. Inoue, N. Ishii, K. Tanaka, Y. Izumi, S. Okamoto. *Displays*, **23**(5), 249 (2002).
[9] Y. Yang, G. Qian, D. Su, Z. Wang, M. Wang. *Chem. Phys. Lett.*, **402**(4–6), 389 (2005).

[10] M. Kandaz, A. Koca, A.R. Özkaya. *Polyhedron*, **23**, 1987 (2004); I. Yılmaz, M. Kandaz, A.R. Özkaya, A. Koca. *Monatsh. Für. Chem.*, **133**, 609 (2002).
[11] I. Gürol, V. Ahsen, Ö. Bekaroğlu. *J. Chem. Soc., Dalton Trans.*, 2283 (1992).
[12] M. Kandaz, I. Yılmaz, S. Keskin, A. Koca. *Polyhedron*, **21**, 825 (2002); M. Kandaz, S.Z. Çoruhlu, I. Yılmaz, A. Koca. *Trans. Met. Chem.*, **27**, 877 (2002).
[13] V. Ahsen, A. Gürek, A. Gül, Ö. Bekaroğlu. *J. Chem. Soc., Dalton Trans.*, 5 (1990).
[14] Y. Gök, H. Kantekin. *J. Coord. Chem.*, **45** (1–4), 15 (1998); H. Kantekin, U. Ocak, Y. Gok, I. Acar. *J. Incl. Phenom.*, **48** (3), 95 (2004).
[15] G. Gümüş, V. Ahsen. *Mol. Cryst. Liq. Cryst.*, **348**, 167 (2000).
[16] K. Ohta, R. Higashi, M.I. Kejima, I. Yamamoto, N. Kobayashi. *J. Mater. Chem.*, **8**, 1979 (1998).
[17] M.J. Prushan, A.W. Addison, R.J. Butcher. *Inorg. Chim. Acta*, **992**, 300 (2000).
[18] M. Kandaz, A.R. Özkaya, A. Cihan. *Trans. Met. Chem.*, **28**, 650 (2003).
[19] V.M. Alexander, R.P. Bhat, S.D. Samant. *Tetrahedron Lett.*, **46**, 6957 (2005).
[20] A. Kilic, E. Tas, B. Gümgüm, I. Yilmaz. *Chin. J. Chem.*, **24** (11), 1599 (2006).; E. Tas, M. Aslanoglu, A. Kilic, Z. Kara. *Trans. Met. Chem.*, **30** (6), 758 (2005).
[21] M. Kurtoglu, E. Ispir, N. Kurtoğlu, S. Toroglu, S. Serin. *Trans. Met. Chem.*, **30**(6), 765 (2005).
[22] A. Para. *Carbohyd. Polym.*, **57**(3), 277 (2004).
[23] S. Soylu, M. Kandaz, N. ÇalıŞkan. *Acta Cryst.*, **E60**, 1348 (2004).
[24] A. Gül, Ö. Bekaroğlu. *J. Chem. Soc., Dalton Trans.*, 2537 (1983).
[25] M. Kandaz, A.R. Özkaya, A. Koca. *Trans. Met. Chem.*, **29**, 847 (2004).
[26] N. Sengottuvelan, J. Manonmani, M. Kandaswamy. *Polyhedron*, **21**, 2767 (2002).
[27] G. Panzio, F. Baldrocca. *Gazz. Chim. Ital.*, **60**, 415 (1930).
[28] H. Brintzinger, R. Titman. *Chem. Ber.*, **85**, 344 (1952).
[29] M. Thimons, C.A. Chua, M. Achalabun. *J. Chem. Ed.*, **75**, 12 (1998).